Available online at www.sciencedirect.com

SciVerse ScienceDirect

Ceramics International 39 (2013) 3555–3561

CERAMICS INTERNATIONAL

www.elsevier.com/locate/ceramint

Phase structure and piezoelectric properties of Ca- and Ba-doped $K_{1/2}Na_{1/2}NbO_3$ lead-free ceramics

J. Taub, L. Ramajo*, M.S. Castro

Institute of Research in Material Science and Technology (INTEMA), (CONICET—Universidad Nacional de Mar del Plata), Juan B Justo 4302 (B7608FDQ), Mar del Plata, Argentina

Received 28 August 2012; received in revised form 7 October 2012; accepted 8 October 2012
Available online 23 October 2012

Abstract

Piezoelectric lead-free ceramics, $K_{1/2}Na_{1/2}NbO_3$ (KNN) modified with alkaline-earth (AE) Ca^{2+} and Ba^{2+}, have been prepared by the conventional solid-state reaction method. The effect of doping level on sinterability and functional response of KNN was studied. In this way, discs doped with 0 to 2 mol% of Ba^{2+} and Ca^{2+} were sintered at 1125 °C for 2 h. It was observed that AE changed drastically the microstructure and grain size of KNN when it was added in concentrations higher than 0.5 mol%. Addition of 0.5 mol% of Ba^{2+} and Ca^{2+} produced a softening effect in the ferroelectric properties of the material, while samples prepared with higher contents than 0.5 mol% showed poor properties.

Keywords: C: Piezoelectric properties and Electrical properties; D: Perovskites and Alkaline earth oxides

1. Introduction

Lead zirconate titanate (PZT) ceramics are widely used materials for piezoelectric applications due to their superior ferroelectric and piezoelectric properties [1–3]. However, the toxicity of lead oxide and its high vapor pressure during the sintering process are a serious threat to human health and environment. Therefore, in recent years lead-free piezoelectric ceramics have attracted a lot of attention.

Potassium sodium niobate $(K_{1-x},Na_x)NbO_3$ ceramics were reported to show good electric properties for piezoelectric application. These ceramics showed low dielectric constant and high electromechanical coupling coefficient [4]. Moreover, better electric properties were obtained when x is 0.5. This composition is reported to be composed of a virtual morphotropic phase boundary, where the total polarization can be maximized due to the increased possibility of domain orientation [5,6]. Nevertheless, because of the high volatility of alkaline metals at high temperature and its hydrophilic feature, it is very difficult to obtain dense and well-sintered KNN ceramics using conventional sintering processes [7]. Since, a deviation from stoichiometry results in the formation of extra phases, a relatively low sintering temperature, and the difficulty of obtaining a fine microstructure during sintering difficult the densification of KNN ceramics [8,9].

To solve this problem several options were studied. In this way, hot pressing could be a good alternative for solving this issue. Although this technique is able to obtain high densities and better properties compared to conventional air-sintered samples, it needs careful investigation and optimization of sintering parameters to result in reproducible and high quality ceramics [10]. Additionally, it is a more expensive route compared to conventional sintering process. Then, the study of different additives to obtain KNN with low porosity and good electrical properties by conventional methods is extremely important.

In this work, the effect of the addition of Ca^{2+} and Ba^{2+} to KNN ($K_{1/2}Na_{1/2}NbO_3$) was investigated. It was expected that both, Ca^{2+} (100 pm ionic radius) and Ba^{2+} (135 pm ionic radius) enter in positions "A" of the perovskite structure producing cationic vacancies to equilibrate the charge which would reduce local stress and

*Corresponding author. Tel.: +54 223 4816600x238.
E-mail address: lramajo@fi.mdp.edu.ar (L. Ramajo).

0272-8842/$ - see front matter © 2012 Elsevier Ltd and Techna Group S.r.l. All rights reserved.
http://dx.doi.org/10.1016/j.ceramint.2012.10.181

consequently produce a "softening" effect in its properties. The ceramic powders were synthesized by the conventional solid state reaction method. The obtained powders were pressed into discs and sintered in air. A microstructural and electrical characterization of powders as well as the sintered samples was carried out.

2. Experimental

Lead-free potassium sodium niobate $K_{1/2}Na_{1/2}NbO_3$ (KNN) modified with Ba and Ca was produced by the conventional solid state reaction method from potassium carbonate (Biopack 99.5%, Argentina), sodium carbonate (Biopack 99.5%, Argentina), niobium oxide powder (Aldrich 99.9%, USA), calcium carbonate (Cicarelli 99.7%, Argentina) and barium carbonate (Aldrich 99.9%, USA). Powders with K:Na = 1:1 and different Ba and Ca concentrations (x = 0, 0.5, 1 and 2 mol%) were mixed in 2-propanol and milled in a planetary laboratory ball-mill (Fritsch, Pulverisette 5), with zirconium oxide grinding jars and balls, for 6 h at 1000 rpm. Afterwards, the resulting powders were calcined at 900 °C for 5 h in air.

The resulting powders were uniaxially pressed into discs of 6 mm diameter and 0.5 mm in thickness. The obtained discs were sintered at 1125 °C for 2 h in a conventional furnace using 5 °C/min heating and cooling rates.

The crystalline phases were assessed by X-ray diffraction using a Philips PW1050/25 diffractometer running with CuK_α radiation, at 40 KV and 30 mA. The microstructure of the samples was examined by Scanning Electron Microscopy (SEM), using a JEOL JSM-6460LV microscope. Raman spectra were acquired at room temperature with a Renishaw inVia Raman spectrometer by means of the 514 nm Ar-ion laser line (10 mW nominal power).

For the electrical measurements, silver electrodes were painted on both faces of the sintered samples. Dielectric properties were measured using a frequency range of 0.10 Hz to 10 MHz employing both Hioki 3535 and 3522-50 LCR meters. Polarization versus electric field hysteresis loops were obtained in a silicone oil bath at room temperature by applying an electric field of sinusoidal waveform at a frequency of 50 Hz by means of a modified Sawyer-Tower bridge. For the measurement of the piezoelectric constant the samples were first polarized inside a silicone bath using 2.5 KV/mm for 30 min at 150 °C, and the piezoelectric coefficients d_{33} were recorded using a quasi-static piezoelectric d_{33} meter (YE2730—Sinoceramics Inc.).

3. Results and discussion

Fig. 1A shows the X-ray diffraction patterns of KNN doped with different concentrations of Ba and Ca (0 to 2 mol%). The diffraction peaks could be clearly indexed to a perovskite with orthorhombic structure of KNN [11–13]. Small peaks corresponding to secondary phases traces were also detected. Secondary phases could be associated

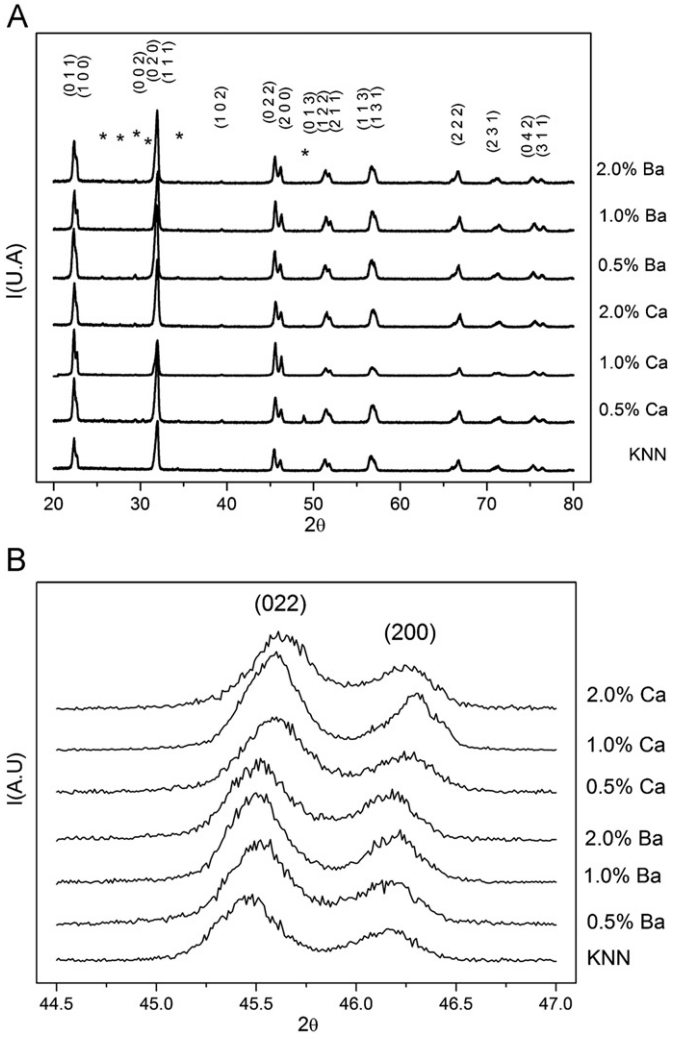

Fig. 1. XRD patterns of KNN undoped (0%) and Ba and Ca-doped samples (0 to 2 mol%). ⁎ Secondary phases ($K_2Nb_8O_{21}$) (JCPDS 031-1060) and K_3NbO_4 (JCPDS 014-0283) (A). The inset shows magnified patterns in the 44.5 to 47° 2θ range (B).

with $K_2Nb_8O_{21}$ (JCPDS 031–1060) and K_3NbO_4 (JCPDS 014–0283), with tetragonal tungsten–bronze structure TTB [14,15]. After analyzing the peaks located between $44.75° < 2\theta < 46.5°$ corresponding to the (022) and (200) planes (Fig. 1B), the coexistence of a rich orthorhombic phase and a poor tetragonal phase in all cases was stablished.

The Raman spectra of the KNN samples doped with Ba and Ca are shown in Fig. 2. This spectroscopic technique is a very sensitive tool to study the structural deformations of the ceramic unit cell at a local scale. In the KNN structures, the main vibrations are associated with the NbO_6^- octahedron (BO_6^-) [16,17]. Therefore, the deformations are induced by the tilting of octahedral and the cationic displacements [18]. These modifications induce large changes in internal modes associated with NbO_6^- octahedron resulting in a modification of the Raman spectra [18]. In this way, it can be seen in Fig. 2A and B that the Raman spectrum peaks relate to the vibrations of

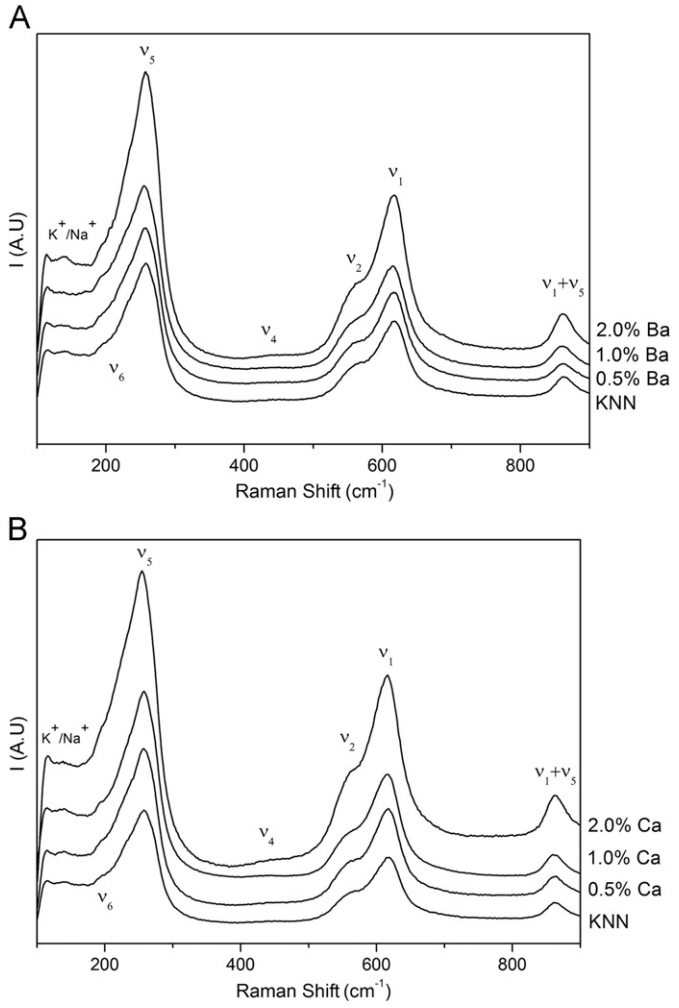

Fig. 2. Raman spectra of KNN undoped (0%) and KNN-doped with (A) Ba and (B) Ca as a function of additive concentration (0 to 2 mol%).

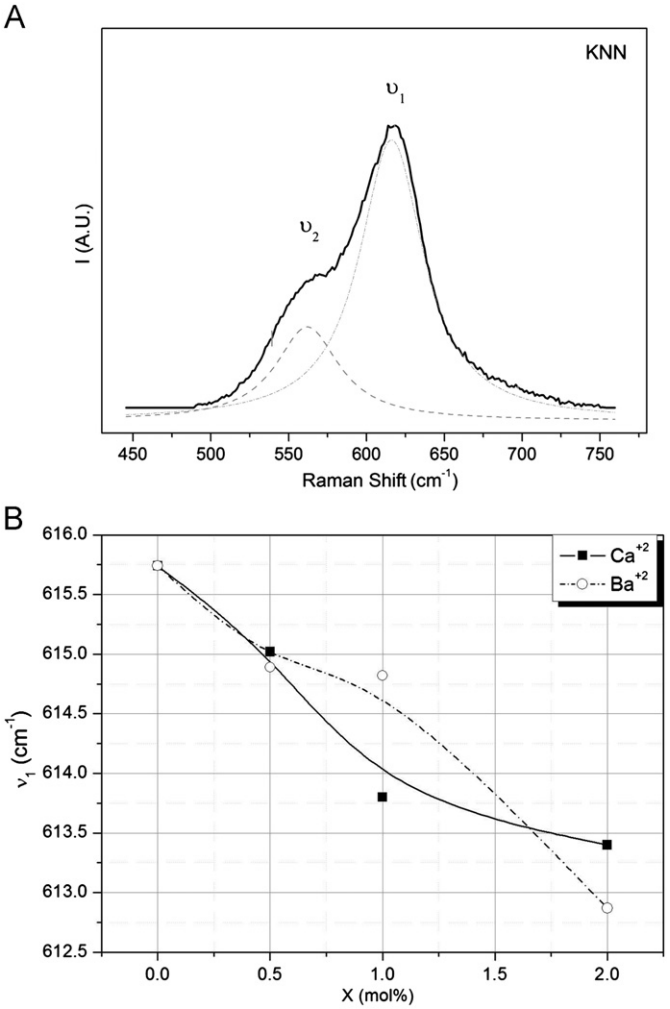

Fig. 3. (A) Representative Gaussian fit of the individual bands of $A_{1\,g}$ (υ_1) and E_g (υ_2) Raman modes of pure KNN in the range of 450 to 760 cm^{-1}. (B) υ_1 Raman modes values obtained after fit as a function of Ca and Ba concentration.

the NbO_6^- octahedron, consisting of $A_{1\,g}(\upsilon_1)+Eg(\upsilon_2)+F_{1\,u}(\upsilon_3, \upsilon_4)+F_{2\,g}(\upsilon_5)+F_{2\,u}(\upsilon_6)$. Vibrations modes $A_{1\,g}(\upsilon_1)+E_g(\upsilon_2)+F_{1\,u}(\upsilon_3)$ are stretching modes and the rest of them are bending modes. In particular, $A_{1\,g}(\upsilon_1)$ and $F_{2\,g}(\upsilon_5)$ have been detected as being relatively strong scatterings in similar systems to the one studied in this paper due to a near-perfect equilateral octahedral symmetry. Finally, the peaks in the region between 100 and 160 cm^{-1} can be associated with translational models of alkaline niobates K^+/Na^+ and rotational modes of the octahedron NbO_6^- [19–21].

Fig. 3A shows representative enlarged Raman spectra of pure KNN between 450 and 760 cm^{-1}. Also, the fit to the sum of two Gaussians ascribed to υ_2 and υ_1 Raman modes, respectively is shown. In Fig. 3B it can be seen that the value of υ_1 decrease when the concentration of dopants increase. This behavior is owe to a decrease in the strength of the constant force that produces a lengthening of the distance between B^{5+} type ions and their coordinated oxygen [22]. It can be attributed to the formation of oxygen vacancies or to a relative increase of the orthorhombic phase. Since the probability of Ca^{2+} and Ba^{2+} ions replacing Nb^{5+} ions (and consequently producing oxygen vacancies) is very low, the observed behavior is attributed to a relative increase in the orthorhombic phase.

In Table 1 it can be seen that the addition of higher concentration than 0.5 mol% for both dopants produces a drastic diminution of the samples density and, consequently, increases the samples porosity. The evolution on the morphology of the microstructure of KNN as a function of Ba and Ca concentration is shown in the Scanning Electron Microscopy images of Fig. 4. Undoped and doped samples with 0.5 mol% of calcium exhibited similar bimodal grain size (~3 μm and ~1 μm), inhomogeneous shape and porosity. The addition of 1 mol% of calcium produces a growth in the cubic grains and a glassy phase. With 2 mol% of Ca, grains grow even more and develop a bimodal grain size (~9 μm and ~3 μm). This behavior might be related to the substitution effect of Ca^{2+} which it is more likely to enter in Na^{1+} position producing cationic vacancies due to their similar ionic radii (100 and 102 pm, respectively). Samples with 0.5 mol% of

Table 1
Density and porosity values, dielectric and piezoelectric properties of KNN pure and Ba- and Ca-doped ceramics.

Sample	Density (g/cm^3)	Porosity (%)	ε' (10 kHz)	tanδ (10 kHz)	d_{33} (pC/N)
KNN pure	4.28 ± 0.19	5.75 ± 2.45	352	0.13	86
KNN 0.5%Ba	4.33 ± 0.07	4.21 ± 1.72	366	0.08	90
KNN 1.0%Ba	4.02 ± 0.08	12.18 ± 2.31	332	0.10	–
KNN 2.0%Ba	4.01 ± 0.07	12.62 ± 2.03	244	0.13	–
KNN 0.5%Ca	4.26 ± 0.08	6.01 ± 1.95	293	0.06	105
KNN 1.0%Ca	4.20 ± 0.06	7.37 ± 1.66	225	0.08	–
KNN 2.0%Ca	4.02 ± 0.15	12.24 ± 4.16	299	0.10	–

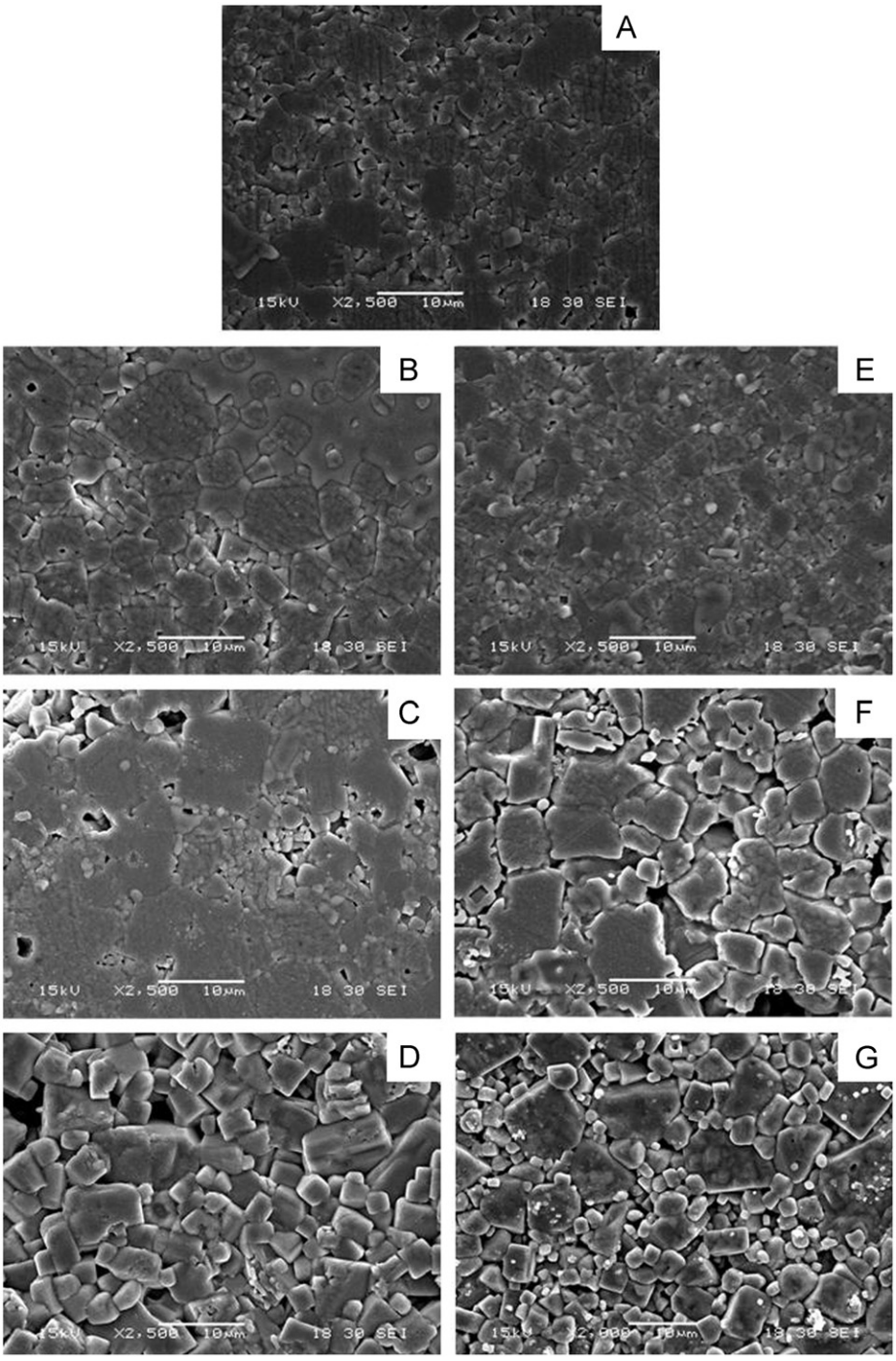

Fig. 4. SEM images of undoped (A); and 0.5 to 2 mol% of Ba-doped KNN ceramics (B, C and D, respectively), and 0.5 to 2 mol% of Ca-doped KNN sample (E, F and G, respectively).

barium present an increase in grain size (~3 μm in average) and a small percentage of glassy phases. When the barium amount is increased, grains grow, as well as, the samples porosity. In both cases, changes in grain sizes and shapes, caused by the addition of higher concentrations than 0.5%mol of dopant, might be related to the ability of segregated potassium ions to produce a glassy secondary phase [23]. This secondary phase facilitates the mass transport and, then, the grain growth. In this case, this behavior might be related to the preferred substitution effect of Ba^{2+} in K^{1+} position, producing cationic vacancies and a high amount of secondary phase, due to their similar ionic radii (135 and 138 pm, respectively). When Ca^{2+} is added, the secondary phase formation is delayed due to the Ca^{2+} tends to replace Na^{1+} at first. The diminution in samples density might be related also to the sodium volatilization.

The real and imaginary parts of permittivity as function of frequency and AE content are shown in Fig. 5. In all cases, it can be seen, at the low frequency range, that real and imaginary permittivity decrease drastically with frequency due to a space charge relaxation process characteristic of polycrystalline samples. In addition it is observed in the high frequency range a relaxation process (at ~5 MHz) associated to dipolar relaxation events [24].

In the Table 1 the values of real permittivity (ε'), dielectric loss ($\tan\delta$) and piezoelectric constant (d_{33}) are shown. The addition of low content dopants produces a decrease in the loss factors and an increase in the piezoelectric constants. In the case of KNN-0.5 mol% Ba the dielectric constant increase, could be related to an increase in the density. This also helps to improve the piezoelectric constant but the formation of a non ferroelectric secondary phase suppresses this effect. Samples with a higher amount of barium presented a diminution in the permittivity values. This behavior could be related to the increment in the porosity values, the secondary phases amount and the orthorrombic/tetragonal ratio. In the case of Ca permittivity values decrease systematically with Ca content, with the exception of the sample with the higher Ca concentration. The diminution in the permittivity values could be related to the reduction in the density values and increment in the secondary phases. The increase in the permittivity value with the highest calcium addition could be associated with a diminution in the orthorhombic/tetragonal ratio and, also, the presence of chemical inhomogeneities should be considered. These inhomogeneities are generally present as polar nanoregions, typical of relaxor systems, or as phase diffusion, characteristic of a polymorphism [23]. On the other hand, an increase in the piezoelectric constant related to the formation of cationic vacancies in samples with 0.5%mol of Ca is observed. With higher concentration of both, Ca and Ba, the porosity of the samples increases and their polarization, previous to piezoelectric measurements, was impeded.

Finally, specimens with low porosity (pure KNN and doped with 0.5 mol% of Ba and Ca), were analyzed under an external strong electric field, exhibiting in all cases

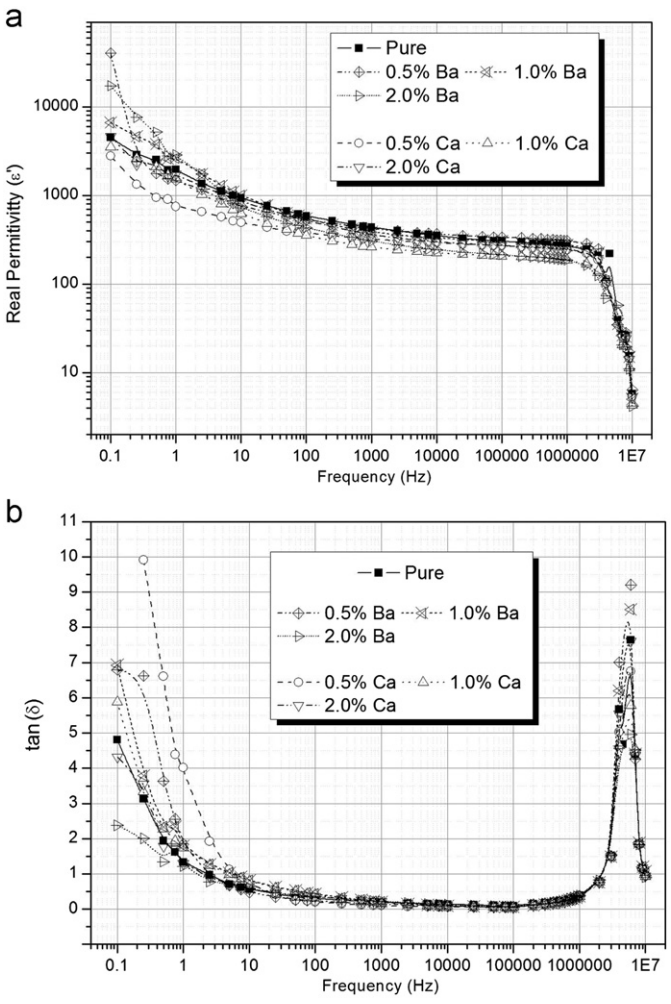

Fig. 5. Variation of (A) real part of permittivity and (B) imaginary permittivity as a function of frequency and Ba and Ca-doped concentration (at room temperature).

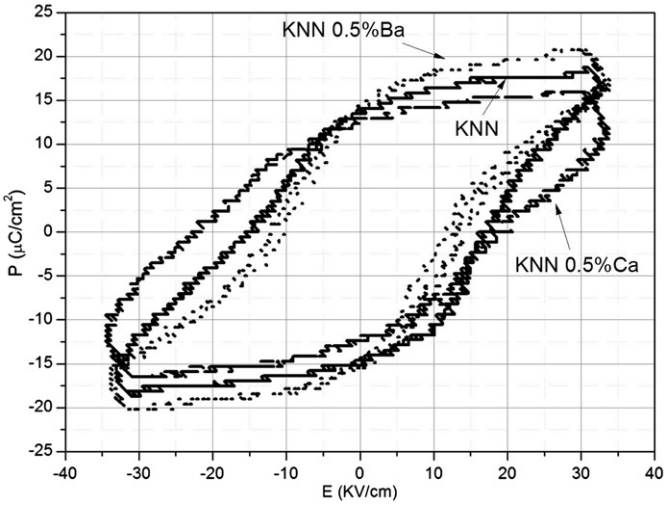

Fig. 6. Hysteresis loops of 0 and 0.5% mol% of Ba and Ca-doped KNN at room temperature. Measuring conditions: *ac* field, electric field of 35 kV/cm and frequency of 50 Hz.

Table 2
Remnant (*Pr*) and saturation (*Ps*) polarizations, and coercive field (*Ec*) of 0 and 0.5% mol% of Ba and Ca-doped KNN at room temperature.

	P_r (μC/cm^2)	*Ec* (KV/cm)	P_s(μC/cm^2)
KNN	13.75	17.3	18.25
KNN 0.5%mol Ca	16	12.4	24.14
KNN 0.5%mol Ba	14.3	12.8	20.08

ferroelectric behavior due to spontaneous polarization. Hysteresis loops of pure and doped KNN at room temperature under an *ac* electric field of $E_p = 35$ kV/cm at 50 Hz are shown in Fig. 6 and Table 2. The coercive field (*Ec*) for pure KNN is higher (17.3 KV/cm) than the one doped with Ca (12.4 KV/cm) and the one doped with Ba (12.8 KV/cm). The area of hysteresis cycle for pure KNN is slightly greater than the others. These behaviors are related to the softening effect of Ca and Ba when they are added in low concentration.

4. Conclusions

The solid solution based on $K_{1/2}Na_{1/2}NbO_3$ (KNN) ceramics was prepared by the conventional solid-state reaction method. KNN ceramics with the aid of 0.5 to 2 mol% of two kind of alkaline-earth, Ba and Ca, were obtained. There was a tendency of Ca^{2+} and Ba^{2+} to enter in "A" sites (Na^+ and K^+ respectively) of the perovskite structure producing cationic vacancies and consequently "softening" the properties of the system. With the increase of dopant addition to the system, Na^+ and K^+ were segregated. Sodium tended to volatilize and to increase the porosity while potassium tended to form a glassy phase. Because of the increase in porosity and secondary phases, properties get deteriorated with the incorporation of high dopant amounts. Samples with the low dopant content (0.5 mol%) showed the best microstructural and electrical properties.

Acknowledgments

This work was supported by Consejo Nacional de Investigaciones Científicas y Técnicas (CONICET), Agencia Nacional de Promoción Científica y Tecnológica (ANPCyT) and Universidad Nacional de Mar del Plata (UNMdP), Argentina. Also, L'Oréal - UNESCO "For Women in Science" Program is acknowledged.

References

[1] E.M. Alkoy, M. Papila, Microstructural features and electrical properties of copper oxide added potassium sodium niobate ceramics, Ceramics International 36 (2010) 1921–1927.
[2] Y. Li, J. Wang, R. Liao, D. Huang, X. Jiang, Synthesis and piezoelectric properties of $K_xNa_{1-x}NbO_3$ ceramic by molten salt method, Journal of Alloys and Compounds 496 (2010) 282–286.
[3] V. Bobnar, J. Bernard, M. Kosec, Relaxorlike dielectric properties and history-dependent effects in the lead-free $K_{0.5}Na_{0.5}NbO_3$–$SrTiO_3$ ceramic system, Applied Physics Letters 85 (2004) 994–996.
[4] B. Malic, J. Bernard, J. Holc, D. Jenko, M. Kosec, Alkaline-earth doping in (K,Na)NbO_3 based piezoceramics, Journal of the European Ceramic Society 25 (2005) 2707–2711.
[5] Y. Saito, H. Takao, T. Tani, T. Nonoyama, K. Takatori, T. Homma, T. Nagoya, M. Nakamura, Lead-free piezoceramics, Nature 432 (2004) 84–87.
[6] E. Ringgaard, T. Wurlitzer, Lead-free piezoceramics based on alkali niobates, Journal of the European Ceramic Society 25 (2005) 2701–2706.
[7] E. Hollenstein, D. Damjanovic, M. Setter, Temperature stability of the piezoelectric properties of Li-modified KNN ceramics, Journal of the European Ceramic Society 27 (2007) 4093–4097.
[8] F. Rubio-Marcos, P. Ochoa, J. Fernadez, Sintering and properties of lead-free (K,Na,Li)(Nb,Ta,Sb)O_3 ceramics, Journal of the European Ceramic Society 27 (2007) 4125–4129.
[9] J. Hao, R. Chu, Z. Xu, G. Zang, G. Li, Structure and electrical properties of (Li, Sr, Sb)-modified $K_{0.5}Na_{0.5}NbO_3$ lead-free piezoelectric ceramics, Journal of Alloys and Compounds 479 (2009) 376–380.
[10] S. Zhang, R. Xia, T. Shrout, G. Zang, J. Wang, Influence of Ni doping on the properties of perovskite molybdates $SrMo_{1-x}Ni_xO_3$ ($0.02 \le x \le 0.08$), Solid State Communications 141 (2007) 675 675.
[11] H. Birol, D. Damjanovic, N. Setter, Preparation and characterization of $(K_{0.5}Na_{0.5})NbO_3$ ceramics, Journal of the European Ceramic Society 26 (2006) 861–866.
[12] B. Malic, J. Bernard, J. Holc, D. Jenko, M. Kosec, Alkaline-earth doping in (K,Na)NbO_3 based piezoceramics, Journal of the European Ceramic Society 25 (2005) 2707–2711.
[13] Y. Chang, Z. Yang, X. Chao, R. Zhang, X. Li, Dielectric and piezoelectric properties of alkaline-earth titanate doped $(K_{0.5}Na_{0.5})NbO_3$ ceramics, Materials Letters 61 (2007) 785–789.
[14] L. Ramajo, M.M. Reboredo, M.S. Castro, Influencia de las condiciones de procesamiento sobre las propiedades dieléctricas y microestructurales de cerámicos de $K_{1/2}Na_{1/2}NbO_3$, Boletín de la Sociedad Española de Cerámica y Vidrio 50 (2011) 9–14.
[15] Y. Wang, J. Wu, D. Xiao, J. Zhu, P. Yu, L. Wu, X. Li, Piezoelectric properties of (Li, Ag, Sb) modified $(K_{0.50}Na_{0.50})NbO_3$ lead-free ceramics, Journal of Alloys and Compounds 462 (2008) 310–314.
[16] N. Klein, E. Hollenstein, D. Damjanovic, H.J. Trodahl, N. Setter, M. Kuball, A study of the phase diagram of (K,Na,Li)NbO_3 determined by dielectric and piezoelectric measurements, and Raman spectroscopy, Journal of Applied Physics 102 (2007) 014112.
[17] K. Kakimoto, K. Akao, Y. Guo, H. Ohsato, Raman scattering study of piezoelectric $(Na_{0.5}K_{0.5})NbO_3$-$LiNbO_3$ ceramics, Japanese Journal of Applied Physics 44 (2005) 7064–7067.
[18] F. Rubio-Marcos, P. Marchet, T. Merle-Méjean, J.F. Fernandez, Role of sintering time, crystalline phases and symmetry in the piezoelectric properties of lead-free KNN-modified ceramics, Materials Chemistry and Physics 123 (2010) 91–97.
[19] Y. Guo, H. Luo, H. Xu, X. Zhou, X. Pan, Z. Yin, Ultra-high piezoelectric response in $<110>$-oriented polydomain $Pb(Mg_{1/3}Nb_{2/3})O_3$–$PbTiO_3$ single crystals, Applied Physics A Materials 77 (2003) 707–709.
[20] Z. Shen, W. Wan, S. Tang, M. Kouk, Raman scattering investigations of the antiferroelectric-ferroelectric phase transition of $NaNbO_3$, Journal of Raman Spectroscopy 29 (1998) 379–384.
[21] R.-C. Chang, S.-Y. Chu, Y.-F. Lin, C.-S. Hong, P.-C. Kao, C.-H. Lu, The effects of sintering temperature on the properties of $(Na_{0.5}K_{0.5})NbO_3$–$CaTiO_3$ based lead-free ceramics, Sensor Actuatuators A-Physics 138 (2007) 355–360.
[22] F. Rubio-Marcos, J.J. Romero, M.S. Martín-Gonzalez, J.F. Fernández, Effect of stoichiometry and milling processes in the synthesis and the piezoelectric properties of modified KNN nanoparticles by solid state reaction, Journal of the European Ceramic Society 30 (2010) 2763–2771.

[23] F. Rubio-Marcos, M.G. Navarro-Rojero, J.J. Romero, P. Marchet, J.F. Fernández, Piezoceramics properties as a function of the structure in the system (K,Na,Li)(Nb,Ta,Sb)O_3, IEEE Transactions on Ultrasonics, Ferroelectrics, and Frequency Control 9 (2009) 1835–1842.

[24] L. Ramajo, R. Parra, M.A. Ramírez, M.S. Castro, Electrical and microstructural properties of $CaTiO_3$-doped $K_{1/2}Na_{1/2}NbO_3$-lead free ceramics, Bulletin of Material and Science 34 (2011) 1213–1217.